Microbial Conjugation Studies of Licochalcones&Xanthohumol

Subjects: Biotechnology & Applied Microbiology

Contributor: Ik-Soo Lee

Microbial conjugation studies of licochalcones (1–4) and xanthohumol (5) were performed by using the fungi *Mucor hiemalis* and *Absidia coerulea*. As a result, one new glucosylated metabolite was produced by *M. hiemalis* whereas four new and three known sulfated metabolites were obtained by transformation with *A. coerulea*. Chemical structures of all the metabolites were elucidated on the basis of 1D-, 2D-NMR and mass spectroscopic data analyses. These results could contribute to a better understanding of the metabolic fates of licochalcones and xanthohumol in mammalian systems. Although licochalcone A 4′-sulfate (7) showed less cytotoxic activity against human cancer cell lines compared to its substrate licochalcone A, its activity was fairly retained with the IC50 values in the range of 27.35–43.07 μM.

Keywords: licochalcones ; xanthohumol ; sulfation ; microbial conjugation

1. Introduction

The licorice root, known as "*Radix Glycyrrhizae*", has been used in traditional Chinese medicines for centuries to treat respiratory infections, gastritis, tremors, and peptic ulcers [1][2]. At present, there are hundreds of compounds isolated from licorice, including flavonoids, triterpene saponins, and alkaloids which are responsible for antidiabetic, neuroprotective, anti-inflammatory, and other bioactive effects [2]. Licochalcones, the significant components of licorice flavonoids, including licochalcone A (LCA, **1**), licochalcone B (LCB, **2**), licochalcone C (LCC, **3**), and so on, were reported to exhibit a variety of bioactivities, and can be used in food and cosmetic industries [2]. In recent years, licochalcones have attracted more attention from research communities due to their anticancer potential against different kinds of cancers, such as breast, lung, and gastric cancers [2][3]. Although the pharmacological activities of licochalcones have been extensively investigated, the metabolic pathway of licochalcones in mammals remains largely unknown. It has been reported that LCA can undergo both phase I and phase II metabolic processes in vitro, with the formation of oxygenated and glucuronidated metabolites [4][5], and the in vivo metabolism studies of LCA led to the determination of glucuronidated, *N*-acetyl-l-cysteine conjugated, and sulfated metabolites [5][6].

In comparison to licochalcones, metabolism of xanthohumol (XN, **5**) (**Figure 1**), a prenylated chalcone from hops, was quite extensively examined and both in vitro and in vivo studies have been conducted. The studies using human and rat liver microsomes resulted in the identification of hydroxylated, cyclized, and glucuronidated metabolites [7][8][9]. In addition, sulfate conjugated metabolites of XN were observed after using sulfotransferases and detected in rats after administration of hop extract [10][11]. However, it seems impossible to identify the conjugation position of the sulfate group by using the LC/MS analysis method without a respective reference compound. It was reported that the phase II enzymes UDP-glucuronosyltransferases and sulfotransferases were not only found in liver but also in other tissues [12], suggesting that LCA and XN could be also metabolized by other organs and tissues.

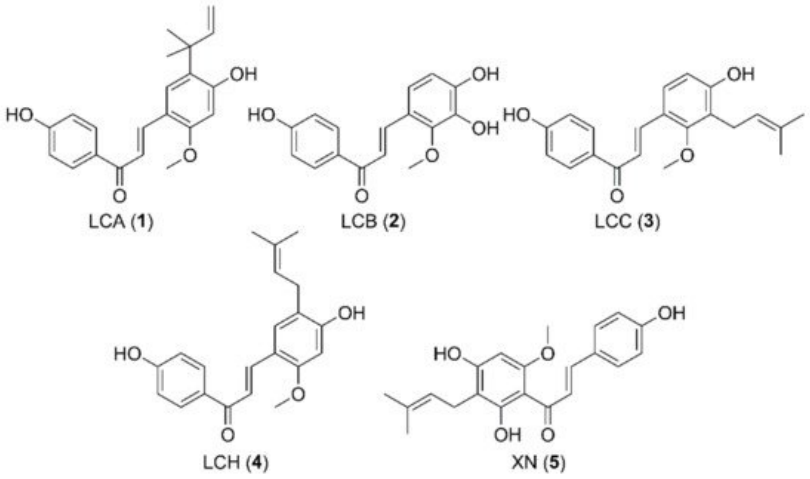

Figure 1. Chemical structures of licochalcones A–C (**1**–**3**), H (**4**) and xanthohumol (**5**).

LCA and XN undergo complex biotransformation processes in mammalian systems and they are mainly metabolized by phase II enzymes, although their interactions with cytochrome P450 enzymes cannot be excluded. Polyphenolic substances are easy targets for conjugation reactions and these are indeed the major biotransformation pathways of licochalcones [13]. Therefore, it is more relevant to investigate the effects of metabolically conjugated derivatives on human health rather than their parent compounds [14]. Generally, sulfate conjugation is considered as a detoxification pathway for endogenous and exogenous phenolic compounds, as the conjugated derivatives are polar and water-soluble, which facilitates their elimination from the body [15][16]. Nevertheless, it is clear today that detoxification is not the only function of sulfation, and the biological activities of compounds after sulfation can be retained, lowered, abolished, or even increased [14][17][18]. For instance, mangostin 3-sulfate exhibited stronger anti-mycobacterial activity against Mycobacterium tuberculosis than α-mangostin [19]. However, compared to the glucuronidated and methylated conjugates, the biological properties and cellular activities of sulfated conjugates were least studied [14]. It is important to expand the structural diversity of sulfated derivatives via chemical or biological methods for biological studies.

2. Microbial Transformation of Licochalcone A and Xanthohumol by *M. hiemalis*

During our previous study, it was observed that licochalcones B, C, H could be *O*-glucosylated by using the fungus *M. hiemalis* [20]. Here, the same process was performed with LCA and XN, which led to the isolation of a new compound licochalcone A 4-*O*-β-D-glucopyranoside (**6**) together with a known compound xanthohumol 4′-*O*-β-D-glucopyranoside [21]. Yin and colleagues discovered a phenolic glycosyltransferase MhGT1 from *M. hiemalis* and applied the enzymatic approach to obtain a series of glycosylated phenolic compounds [22]. Likewise, the *O*-glucosylation process observed here was speculated to be catalyzed by the enzyme glycosyltransferase formed by *M. hiemalis*.

Compound **6** was isolated as an orange amorphous powder. HRESIMS of **6** exhibited a quasi-molecular ion at m/z 523.1943 $[M+Na]^+$ (calcd. for C27H32O9Na, 523.1944), suggesting the molecular formula of **6** as C27H32O9, which was one glucose unit higher than that of **1**. The presence of sugar moiety was further confirmed by comparison of its NMR spectra with those of **1**, which showed an anomeric proton signal at δH 5.01 (1H, d, J = 7.0 Hz) in ^{1}H-NMR spectrum and a hexose carbon signals at δC (100.5, 73.8, 77.8, 70.7, 78, and 61.4) in ^{13}C-NMR. The significant downfield-shifted proton signal of H-3 in ring B indicated that the glucose moiety was attached to 4-OH. HMBC correlation from the anomeric proton signal at δH 5.01 (H-1‴) to the carbon signal at δC 159.4 (C-4) confirmed the assignment of glycosylation at C-4 (**Figure 2**). The resonances of the glucose moiety were assigned by HSQC and HMBC experiments (See Supplementary Materials). TLC comparison with the authentic sample after acid hydrolysis of **6** led to the elucidation of the glucose moiety to be d-form [21][23]. The aglycone part of the ^{1}H- and ^{13}C-NMR spectra of **6** revealed two sets of signals in the integral ratio of around 1:1.3. Based on the two pairs of H-α and H-β proton signals at δH 7.67 (1H, d, J = 15.7 Hz) and 7.92 (1H, d, J = 15.7 Hz), together with δH 6.44 (1H, d, J = 12.8 Hz) and 7.03 (1H, d, J = 12.8 Hz), **6** was clearly assigned as a mixture of trans- and cis-isomers. Based on the above data and extensive 2D NMR experiments, structure of the compound **6** was assigned as licochalcone A 4-*O*-β-D-glucopyranoside.

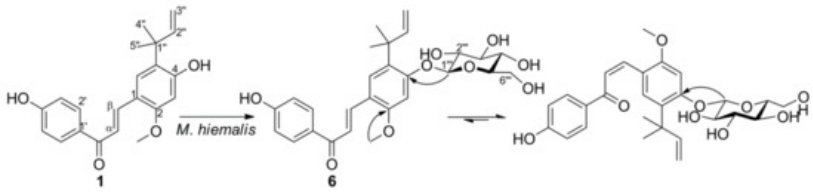

Figure 2. Microbial transformation of **1** by *M. hiemalis*. Selected HMBC correlations ($^{1}H \rightarrow {}^{13}C$) of metabolite **6** are indicated by arrows.

3. Microbial Transformation of Licochalcones A, B, C, H, and Xanthohumol by *A. coerulea*

Screening of licochalcones and XN (**1**–**5**) with several microorganisms showed that only *A. coerulea* was able to produce the highly polar metabolites, more polar than the metabolites transformed by *M. hiemalis*. During the screening procedures, it was also observed that by using more sulfate-containing media, the yield of sulfate-conjugated metabolites could be increased. Thus, instead of using the original incubation medium suggested by KCTC, the scale-up fermentation process was performed by using a modified Czapek Dox media (dextrose 10 g/L, sodium nitrate 2 g/L, dipotassium phosphate 1 g/L, magnesium sulfate 0.5 g/L, potassium chloride 0.5 g/L, ferrous sulfate 0.02 g/L). Isolation of the metabolites from large-scale fermentations was processed successfully by using EtOAc as extraction solvent.

Metabolite **7** was isolated as a yellow amorphous powder. The UV spectrum showed maximum absorption bands at 266 and 387 nm, similar to those of substrate **1**. The HRESIMS spectra of **7** displayed a molecular ion peak at *m/z* 417.1024 $[M-H]^-$ and a fragment ion peak at *m/z* 337.1449 $[M-H-80]^-$, suggesting the presence of a sulfate group. In addition, the isotopic mass peak at *m/z* 419.1087 $[M-H+2]^-$ indicated the presence of a sulfur atom in the compound. The IR spectrum of **7** showed the presence of two strong bands corresponding to the S=O (1251 cm^{-1}) and C-O-S (1050 cm^{-1}), supporting the presence of a sulfate group [24]. The presence of the sulfate group was further supported by the formation of white precipitate after treating the aqueous layer of acid-hydrolyzed **7** with BaCl2 [24]. Comparison of the ^{1}H- and ^{13}C-NMR spectroscopic data of **7** with **1** revealed the resonance signals being almost identical in both compounds, except for the downfield shift of H-3′/5′, C-1′, C-3′/5′ (0.44, 4.0, and 4.7 ppm, respectively) and the upfield shift of C-4′ (4.4 ppm), implying that the sulfate moiety was conjugated with 4′-OH. These shifts were consistent with naringenin 4′-sulfate, a transformed product of naringenin, because the carbon directly attached to the sulfate ester and the carbons in the meta-position are upfield-shifted, and the protons and carbons in ortho- and para-positions to the sulfate group are downfield-shifted [18][25]. The sulfate position at C-4′ was further confirmed by HMBC correlations of H-3′/5′ with C-1′ and C-4′ (**Figure 3**). Therefore, the structure of **7** was identified as licochalcone A 4′-sulfate.

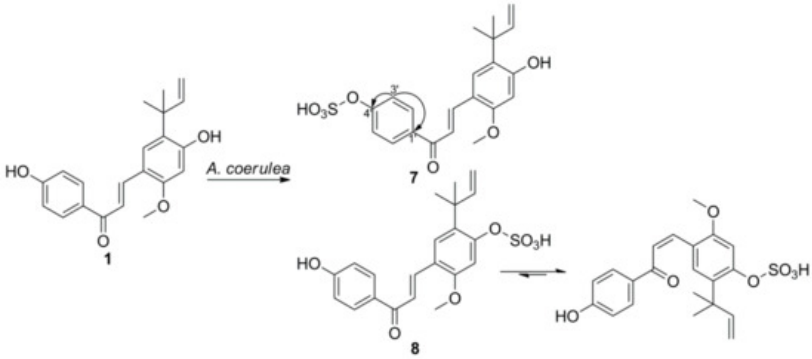

Figure 3. Microbial transformation of **1** by A. coerulea. Selected HMBC correlations ($^{1}H \rightarrow {}^{13}C$) of metabolite **7** are indicated by arrows.

Metabolite **8** was obtained as a mixture with **7**. In the ^{1}H-NMR spectrum of **8**, the significant downfield-shifted signal at δH 7.51 (H-3) was observed, indicating that the sulfate group was attached to 4-OH. Two sets of proton resonance signals were observed for **8**, which is similar to the glucosylated metabolite **6**. Thus, the structure of **8** was identified as *trans*- and *cis*-isomers of licochalcone A 4-sulfate.

Metabolite **9** was obtained as a yellow solid. The HRESIMS spectra of **9** exhibited a molecular ion peak at *m/z* 365.0336 $[M-H]^-$ and a fragment ion peak at *m/z* 285.0767 $[M-H-80]^-$, suggesting the presence of a sulfate group. The ^{1}H-NMR data of **9** were similar to **2**, except for the H-6 signal, which was downfield-shifted by 0.33 ppm. Comparison of ^{13}C-NMR data of **9** and substrate **2** showed that the C-3 signal was upfield-shifted by 5.7 ppm, and the signals of C-2, C-4, and C-6 were downfield-shifted by 4.1, 3.2, and 5.0 ppm, respectively [26]. All of these suggested that the sulfate group was attached to

3-OH, and this was further confirmed by the HMBC correlations between H-5 and C-1/3 (**Figure 4**). Thus, the structure of **9** was identified as licochalcone B 3-sulfate.

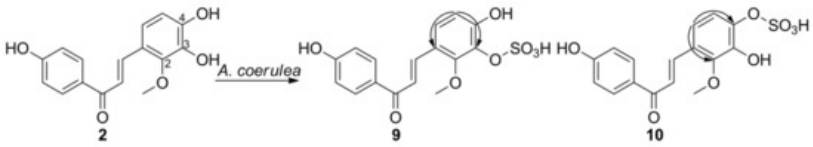

Figure 4. Microbial transformation of **2** by A. coerulea. Selected HMBC correlations ($^{1}H \rightarrow {}^{13}C$) of metabolites **9** and **10** are indicated by arrows.

Metabolite **10** was obtained as a mixture with **9**. In the ^{1}H-NMR spectrum of **10**, the significant downfield-shifted signal at δH 7.22 (H-5) was observed, indicating that the sulfate group was attached to 4-OH. This was supported by the deshielding of C-3 and C-5 carbons, which are ortho to the sulfate site, compared to those of substrate **2** in the ^{13}C NMR of **10** by 3.0 and 5.2 ppm, respectively. Furthermore, the para carbon at C-1 in **10** was deshielded by 4.0 ppm, while the *ipso* carbon at C-4 position was shielded by 7.7 ppm [26]. Based on the above analysis, the structure of **10** was identified as licochalcone B 4-sulfate. The resonances of **10** were completely assigned by HSQC and HMBC spectra (See Supplementary Materials).

Metabolite **11** was obtained as a yellow solid. The HRESIMS spectra of **11** exhibited a molecular ion peak at *m/z* 417.1010 $[M-H]^-$ and a fragment ion peak at *m/z* 337.1438 $[M-H-80]^-$, suggesting the presence of a sulfate group. Two sets of signals in the integral ratio of around 1:1.1 were observed in the ^{1}H- and ^{13}C-NMR spectra of **11**. It was assigned as a mixture of trans- and cis-isomers according to the two pairs of H-α and H-β proton signals at δH 7.73 (1H, d, J = 15.9 Hz) and 8.01 (1H, d, J = 15.9 Hz), together with δH 6.65 (1H, d, J = 12.9 Hz) and 7.10 (1H, d, J = 12.9 Hz). Comparison of the ^{1}H-NMR spectrum of LCC sulfate **11** with the parent compound **3** clearly showed a strong difference in the chemical shift for H-5 in ring B, whereas the chemical shifts of protons in ring A were only slightly changed, suggesting that the sulfate moiety was attached to 4-OH. This was supported by the significant upfield-shifted signal of C-4 and downfield-shifted signals of C-1, C-3, and C-5 in the ^{13}C-NMR spectra of **11** compared with those of **3** [26]. The HMBC correlations between H-6 and C-4, C-2 further confirmed the attachment at C4-OH (**Figure 5**). Thus, the structure of **11** was identified as licochalcone C 4-sulfate.

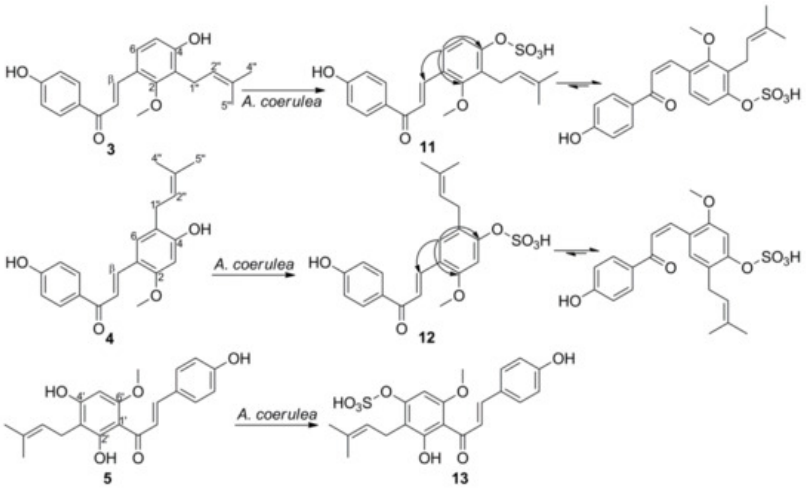

Figure 5. Microbial transformation of **3**–**5** by A. coerulea. Selected HMBC correlations ($^{1}H \rightarrow {}^{13}C$) of metabolites **11** and **12** are indicated by arrows.

Metabolite **12** was obtained as a yellow solid. The HRESIMS spectra of **12** exhibited a molecular ion peak at *m/z* 417.0974 $[M-H]^-$ and a fragment ion peak at *m/z* 96.9881, suggesting the presence of a sulfate group. Two sets of signals in the integral ratio of around 1:1.2 were observed in the ^{1}H- and ^{13}C-NMR spectra of **12**. It was assigned as a mixture of *trans*- and *cis*-isomers, according to the two pairs of H-α and H-β proton signals at δH 7.68 (1H, d, J = 15.8 Hz) and 7.98 (1H, d, J = 15.8 Hz), together with δH 6.43 (1H, d, J = 12.8 Hz) and 7.12 (1H, d, J = 12.8 Hz). Comparison of the ^{1}H-NMR spectrum of LCH sulfate **12** with the parent compound **4** clearly showed a strong difference in the chemical shift for H-3 in ring B, whereas the chemical shifts of protons in ring A were only slightly changed, suggesting that the sulfate moiety was attached to 4-OH. This was supported by the significant upfield-shifted signal of C-4 and downfield-shifted signals of C-1, C-3, and C-5 in the ^{13}C-NMR spectra of **12** compared with those of **4** [27]. Thus, the structure of **12** was identified as licochalcone H 4-sulfate. The resonances of **12** were completely assigned by HSQC and HMBC spectra (See Supplementary Materials).

Metabolite **13** was isolated as a yellow amorphous powder. The HRESIMS spectra of **13** displayed a molecular ion peak at *m/z* 433.1092 $[M-H]^-$ and a fragment ion peak at *m/z* 353.1355 $[M-H-80]^-$, suggesting the presence of a sulfate group. Comparison of the ^{1}H- and ^{13}C-NMR spectroscopic data of **13** with **5** indicated almost identical resonances for both compounds, except for the downfield-shift of H-5′, C-1′, C-3′, C-5′ (0.88, 3.2, 6.0, and 4.7 ppm, respectively) and the upfield-shift of C-4′ (5.8 ppm), implying that the sulfate moiety was conjugated with 4′-OH [28]. Therefore, the structure of **13** was identified as xanthohumol 4′-sulfate.

It has been reported that chalcones can undergo trans to cis transformation in solution when light exposure is available. The presence of a free hydroxyl group at the C-4 position of chalcones inhibits photoisomerization between the *trans*- and *cis*-isomers, as the hydroxyl group at C-4 position enables keto-enol tautomerization and free rotation around the α,β-bond, which allows the rapid conversion of cis chalcones to the stable trans-isomers [4]. The electron-donating group at C-4 position is expected to weaken the α,β-double bond of chalcones through electron-delocalization effects (**Figure 6**), thus the electron-withdrawing effects carried out by the glucose and sulfate moieties of **6**, **8**, **11,** and **12** may quench the electron-donating capacity of the *O*-atom at C-4 [29]. As a result, glucosylation and sulfation of C4-OH raise the barrier and make the cis-trans chalcone isomerization a slow kinetically distinct process [29]. As demonstrated with the isolated metabolites **6**, **11**, and **12**, the ratio of cis- to trans-isomers was found to be >1 in the NMR solvent, suggesting that the cis isomer produced here is structurally stable under the observed conditions [30]. Such observations are quite remarkable in this case as it is commonly known that *trans* chalcones are more stable than their *cis*-isomers.

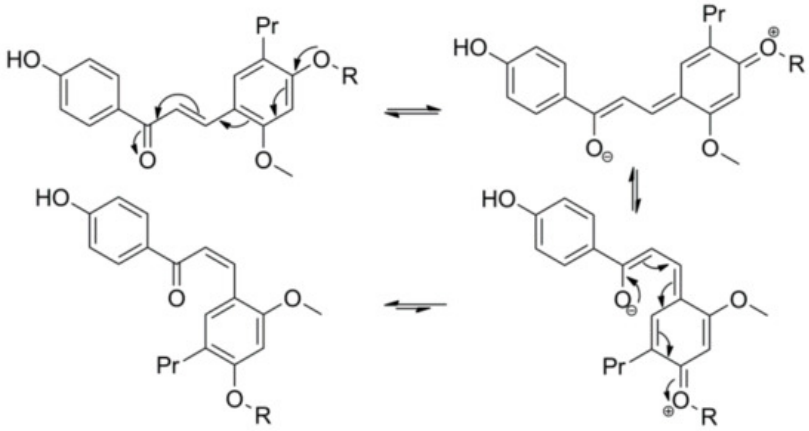

Figure 6. The proposed mechanism of trans-cis isomerization.

The conjugation reactions are widely known as major metabolic pathways for the detoxification of xenobiotic compounds [15]. The conjugated derivatives are more polar and water-soluble and therefore more easily excreted from the body through urine or feces [14][31]. However, an increasing amount of evidence suggests that detoxification is not the only role of sulfation in the organisms. Sulfation might change the biological activities of numerous compounds, and some of the sulfated compounds work therapeutically against cancer, diabetes, and various metabolic diseases [18][32]. A demonstration of parallelism between mammalian and microbial systems, conjugation reaction is of considerable importance for the drug metabolism investigations. However, sulfation in microbial systems is rare and reports on this topic are limited. So far, in addition to the list of microorganisms reported by Khan [33][34][35][36][37], several fungi including *Absidia coerulea* [38], *Colletotrichum gloeosporioides* [19], *Cunninghamella elegans* [25], *Gliocladium deliquescens* [39], *Mucor hiemalis* [40], *Mucor sp*. [41], *Neosartorya spathulata* [19], *Streptomyces fulvissimus*, *Syncephalastrum racemosum* [42], and *Trichothecium roseum* [43] were reported to perform sulfation of some phenolic compounds.

Unlike the complicated sulfation procedure of 8-prenylnaringein, which requires a two-step process with the use of a phosphate buffer [42], we obtained the sulfated metabolites of licochalcones and xanthohumol (**7**–**13**) by directly using the cultures of *A. coerulea*. The metabolite **7** was previously identified as a phase II sulfate conjugate of LCA during the metabolism studies using human hepatocytes [5]. Results obtained from this study showed that *A. coerulea* is capable of sulfation of chalcones and exhibits parallels between microbial and mammalian metabolism not only in phase I but also in phase II metabolism [42][24]. It is widely known that the phase II sulfation reactions are mediated by the enzyme sulfotransferases, which catalyze the transfer of sulfonate group from the active sulfate to the substrates containing hydroxyl groups [44]. Thus, the sulfate metabolites of licochalcones and xanthohumol were supposed to be produced by the enzyme sulfotransferase from *A. coeralea*.

To demonstrate the biological activity of compounds **7**, **13** and their aglycones (**1**, **5**), the cytotoxic activities against three different human cancer cell lines were evaluated by using MTT assay (**Table 1**). Although, as expected, the sulfated metabolites were less active than their aglycones, they still exhibited moderate cytotoxic activities. The glucosylated metabolites displayed weak cytotoxic activity with IC50 > 100 μM. From the results obtained (**Table 1** and Table S1), it was observed that all of the test compounds, except LCC, exhibited higher cytotoxic activities against A375P cells than MCF-7 and A549 cells. LCC showed stronger activity against MCF-7 cells than A549 cells, which was supported by the result reported by Zheng and colleagues [45]. Zheng and colleagues observed that LCB (**2**) exhibited weak cytotoxic activity against MCF-7 cells with IC50 > 80 μM after 24 and 48 h treatment [46], which was similar to our result (Supporting Table S1). All the compounds tested displayed much stronger cytotoxic activities than LCB, indicating that the prenyl group plays a significant role in the cytotoxic activity of these compounds against the tested cancer cell lines. However, Shim and colleagues have reported that LCB exhibited moderate activities against A375 and A431 skin cancer cells (IC50 13.7 and 19.1 μM, respectively) [47], and showed stronger cytotoxic activity against HSC4 oral squamous cell carcinoma cells (IC50 13 μM) than LCA (IC50 20.42 μM), LCC (IC50 27.1 μM), and LCH (IC50 14.4 μM) after 48 h treatment [48][49][50][51]. Though LCA and XN exhibited good activity in most cases, they were found to show low cytotoxic and apoptotic activity against LNCaP prostate cancer cells [52]. Thus, the cytotoxic activity of compounds against different types of cancer cell lines should be evaluated on a case-by-case basis.

Table 1. Cytotoxic activities of compounds against cancer cell lines.

Compound	Cell Lines (IC50, μM)		
	A375P	MCF-7	A549
1	**12.86 ± 3.42**	**19.16 ± 0.65**	**18.14 ± 1.26**
5	**11.02 ± 2.09**	**23.11 ± 1.36**	**26.93 ± 1.56**
7	**27.35 ± 1.44**	**30.85 ± 4.58**	**43.07 ± 1.63**
13	**41.04 ± 1.61**	**81.27 ± 3.05**	**99.40 ± 1.99**
DZ [1]	**9.86 ± 0.57**	**5.12 ± 0.44**	**4.01 ± 0.78**

[1] Used as positive control.

References

1. Maria Pia, G.D.; Sara, F.; Mario, F.; Lorenza, S. Biological effects of licochalcones. Mini Rev. Med. Chem. 2019, 19, 647–656.
2. Wang, C.; Chen, L.; Xu, C.; Shi, J.; Chen, S.; Tan, M.; Chen, J.; Zou, L.; Chen, C.; Liu, Z.; et al. A comprehensive review for phytochemical, pharmacological, and biosynthesis studies on Glycyrrhiza spp. Am. J. Chin. Med. 2020, 48, 1–29.
3. Weng, Q.; Chen, L.; Ye, L.; Lu, X.; Yu, Z.; Wen, C.; Chen, Y.; Huang, G. Determination of licochalcone A in rat plasma by UPLC-MS/MS and its pharmacokinetics. Acta Chromatogr. 2019, 31, 262–265.
4. Nadelmann, L.; Tjørnelund, J.; Hansen, S.H.; Cornett, C.; Sidelmann, U.G.; Braumann, U.; Christensen, E.; Christensen, S.B. Synthesis, isolation and identification of glucuronides and mercapturic acids of a novel antiparasitic agent, licochalcone A. Xenobiotica 1997, 27, 667–680.
5. Huang, L.; Nikolic, D.; van Breemen, R.B. Hepatic metabolism of licochalcone A, a potential chemopreventive chalcone from licorice (Glycyrrhiza inflata), determined using liquid chromatography-tandem mass spectrometry. Anal. Bioanal. Chem. 2017, 409, 6937–6948.
6. Nadelmann, L.; Tjørnelund, J.; Christensen, E.; Hansen, S.H. High-performance liquid chromatographic determination of licochalcone A and its metabolites in biological fluids. J. Chromatogr. B Biomed. Sci. Appl. 1997, 695, 389–400.
7. Yilmazer, M.; Stevens, J.F.; Buhler, D.R. In vitro glucuronidation of xanthohumol, a flavonoid in hop and beer, by rat and human liver microsomes. FEBS Lett. 2001, 491, 252–256.
8. Yilmazer, M.; Stevens, J.F.; Deinzer, M.L.; Buhler, D.R. In vitro biotransformation of xanthohumol, a flavonoid from hops (Humulus lupulus), by rat liver microsomes. Drug Metab. Dispos. 2001, 29, 223–231.
9. Nikolic, D.; Li, Y.; Chadwick, L.R.; Pauli, G.F.; van Breemen, R.B. Metabolism of xanthohumol and isoxanthohumol, prenylated flavonoids from hops (Humulus lupulus L.) by human liver microsomes. J. Mass Spectrom. 2005, 40, 289–

299.

10. Ruefer, C.E.; Gerhäuser, C.; Frank, N.; Becker, H.; Kulling, S.E. In vitro phase II metabolism of xanthohumol by human UDP-glucuronosyltransferases and sulfotransferases. Mol. Nutr. Food Res. 2005, 49, 851–856.
11. Jirásko, R.; Holčapek, M.; Vrublová, E.; Ulrichová, J.; Šimánek, V. Identification of new phase II metabolites of xanthohumol in rat in vivo biotransformation of hop extracts using high-performance liquid chromatography electrospray ionization tandem mass spectrometry. J. Chromatogr. A 2010, 1217, 4100–4108.
12. Böhmdorfer, M.; Szakmary, A.; Schiestl, R.H.; Vaquero, J.; Riha, J.; Brenner, S.; Thalhammer, T.; Szekeres, T.; Jäger, W. Involvement of UDP-glucuronosyltransferases and sulfotransferases in the excretion and tissue distribution of resveratrol in mice. Nutrients 2017, 9, 1347.
13. Marhol, P.; Hartog, A.F.; van der Horst, M.A.; Wever, R.; Purchartová, K.; Fuksová, K.; Kuzma, M.; Cvačka, J.; Křen, V. Preparation of silybin and isosilybin sulfates by sulfotransferase from Desulfitobacterium hafniense. J. Mol. Catal. B. Enzym. 2013, 89, 24–27.
14. Sak, K. Chapter 6-Anticancer action of sulfated flavonoids as phase II metabolites. In Handbook of Food Bioengineering, Food Bioconversion; Grumezescu, A.M., Holban, A.M., Eds.; Academic Press: Cambridge, MA, USA; Elsevier Ltd.: Amsterdam, The Netherlands, 2017; Volume 2, pp. 207–236.
15. Koizumi, M.; Shimizu, M.; Kobashi, K. Enzymatic sulfation of quercetin by arylsulfotransferase from a human intestinal bacterium. Chem. Pharm. Bull. 1990, 38, 794–796.
16. Correia-da-Silva, M.; Sousa, E.; Pinto, M.M.M. Emerging sulfated flavonoids and other polyphenols as drugs: Nature as an inspiration. Med. Res. Rev. 2014, 34, 223–279.
17. Roubalová, L.; Purchartová, K.; Papoušková, K.; Vacek, J.; Křen, V.; Ulrichová, J.; Vrba, J. Sulfation modulates the cell uptake, antiradical activity and biological effects of flavonoids in vitro: An examination of quercetin, isoquercitrin and taxifolin. Bioorg. Med. Chem. 2015, 23, 5402–5409.
18. Teles, Y.C.F.; Souza, M.S.R.; de Souza, M.F.V. Sulphated flavonoids: Biosynthesis, structures, and biological activities. Molecules 2018, 23, 480.
19. Arunrattiyakorn, P.; Suksamrarn, S.; Suwannasai, N.; Kanzaki, H. Microbial metabolism of α-mangostin isolated from Garcinia mangostana L. Phytochemistry 2011, 72, 730–734.
20. Xiao, Y.; Han, F.; Lee, I.-S. Microbial transformation of licochalcones. Molecules 2020, 25, 60.
21. Kim, H.J.; Lee, I.-S. Microbial metabolism of the prenylated chalcone xanthohumol. J. Nat. Prod. 2006, 69, 1522–1524.
22. Feng, J.; Zhang, P.; Cui, Y.; Li, K.; Qiao, X.; Zhang, Y.T.; Li, S.M.; Cox, R.J.; Wu, B.; Ye, M.; et al. Regio- and stereospecific O-glycosyation of phenolic compounds catalyzed by a fungal glycosyltransferases from Mucor hiemalis. Adv. Synth. Catal. 2017, 359, 995–1006.
23. Han, F.; Lee, I.-S. A new flavonol glycoside from the aerial parts of Epimedium koreanum Nakai. Nat. Prod. Res. 2017, 33, 320–325.
24. Ibrahim, A.-R.S. Sulfation of naringenin by Cunninghamella elegans. Phytochemistry 2000, 53, 209–212.
25. Ibrahim, A.-R.S.; Galal, A.M.; Ahmed, M.S.; Mossa, G.S. O-Demethylation and sulfation of 7-methoxylated flavonones by Cunninghamella elegans. Chem. Pharm. Bull. 2003, 51, 203–206.
26. Kajiyama, K.; Demizu, S.; Hiraga, Y.; Kinoshita, K.; Koyama, K.; Takahashi, K.; Tamura, Y.; Okada, K.; Kinoshita, T. Two prenylated retrochalcones from Glycyrrhiza inflata. Phytochemistry 1992, 31, 3229–3232.
27. Wang, Z.; Cao, Y.; Paudel, S.; Yoon, G.; Cheon, S.H. Concise synthesis of licochalcone C and its regioisomer, licochalcone H. Arch. Pharm. Res. 2013, 36, 4132–4136.
28. Chen, Q.-H.; Fu, M.-L.; Chen, M.-M.; Liu, J.; Liu, X.-J.; He, G.-Q.; Pu, S.-C. Preparative isolation and purification of xanthohumol from hops (Humulus lupulus L.) by high-speed counter-current chromatography. Food Chem. 2012, 132, 619–623.
29. Basílio, N.; Bittar, S.A.; Mora, N.; Dangles, O.; Pina, F. Analogs of natural 3-deoxyanthocyanins: O-glucosides of the 4′,7-dihydroxyflavylium ion and the deep influence of glycosidation on color. Int. J. Mol. Sci. 2016, 17, 1751.
30. Simmler, C.; Lankin, D.C.; Nikolić, D.; van Breemen, R.B.; Pauli, G.F. Isolation and structural characterization of dihydrobenzofuran congers of licochalcone A. Fitoterapia 2017, 121, 6–15.
31. Correia, M.S.P.; Lin, W.; Aria, A.J.; Jain, A.; Globisch, D. Rapid preparation of a large sulfated metabolite library for structure validation in human samples. Metabolites 2020, 10, 415.
32. Van der Horst, M.A.; Hartog, A.F.; El Morabet, R.; Marais, A.; Kircz, M.; Wever, R. Enzymatic sulfation of phenolic hydroxy groups of various plant metabolites by an arylsulfotransferase. Eur. J. Org. Chem. 2015, 2015, 534–541.

33. Herath, W.; Mikell, J.R.; Hale, A.L.; Ferreira, D.; Khan, I.A. Microbial metabolism part 9. Structure and antioxidant significance of the metabolites of 5,7-dihydroxyflavone (chrysin), and 5- and 6-hydroxyflavones. Chem. Pharm. Bull. 2008, 56, 418–422.
34. Mikell, J.R.; Khan, I.A. Bioconversion of 7-hydroxyflavanone: Isolation, characterization and bioactivity evaluation of twenty-one phase I and phase II microbial metabolites. Chem. Pharm. Bull. 2012, 60, 1139–1145.
35. Ibrahim, A.K.; Radwan, M.M.; Ahmed, S.A.; Slade, D.; Ross, S.A.; ElSohly, M.A.; Khan, I.A. Microbial metabolism of cannflavin A and B isolated from Cannabis sativa. Phytochemistry 2010, 71, 1014–1019.
36. Mikell, J.R.; Herath, W.; Khan, I.A. Microbial metabolism. Part 12. Isolation, characterization and bioactivity evaluation of eighteen microbial metabolites of 4′-hydroxyflavanone. Chem. Pharm. Bull. 2011, 59, 692–697.
37. Herath, W.; Khan, I.A. Microbial metabolism. Part 13. Metabolites of hesperetin. Bioorg. Med. Chem. Lett. 2011, 21, 5784–5786.
38. Bartmańska, A.; Tronina, T.; Huszcza, E. Transformation of 8-prenylnaringenin by Absidia coerulea and Beauveria bassiana. Bioorg. Med. Chem. Lett. 2012, 22, 6451–6453.
39. Fan, N.; Du, C.H.; Xu, J.Q.; Xu, Y.X.; Yu, B.Y.; Zhang, J. Glycosylation and sulfation of 4-methylumbelliferone by Gliocladium deliquescens NRRL 1086. Appl. Biochem. Microbiol. 2017, 53, 85–93.
40. Feng, J.; Liang, W.; Ji, S.; Qiao, X.; Zhang, Y.; Yu, S.; Ye, M. Microbial transformation of isoangustone A by Mucor hiemalis CGMCC 3.14114. J. Chin. Pharm. Sci. 2015, 24, 285–291.
41. Ruan, F.; Chen, R.; Li, J.; Zhang, M.; Xie, K.; Wang, Y.; Feng, R.; Dai, J. Sulfation of naringenin by Mucor sp. Zhongguo Zhongyao Zazhi 2014, 39, 2039–2042.
42. Bartmańska, A.; Tronina, T.; Huszcza, E. Microbial sulfation of 8-prenylnaringenin. Z. Naturforsch 2013, 68c, 231–235.
43. Yuan, W.; Zhang, L.-P.; Cheng, K.-D.; Zhu, P.; Wang, Q.; He, H.-X.; Zhu, H.-X. Microbial O-demethylation, hydroxylation, sulfation, and ribosylation of a xanthone derivative from Halenia elliptica. J. Nat. Prod. 2006, 69, 811–814.
44. Xie, L.; Xiao, D.; Wang, X.; Wang, C.; Bai, J.; Yue, Q.; Yue, H.; Li, Y.; Molnár, I.; Xu, Y.; et al. Combinatorial biosynthesis of sulfated benzenediol lactones with a phenolic sulfotransferase from Fusarium graminearum PH-1. mSphere 2020, 5, e00949-20.
45. Wang, P.; Yuan, X.; Wang, Y.; Zhao, H.; Sun, X.; Zheng, Q. Licochalcone C induces apoptosis via B-cell lymphoma 2 family proteins in T24 cells. Mol. Med. Rep. 2015, 12, 7623–7628.
46. Liu, Y.; Wang, Y.; Yan, X.; Si, L.; Cao, C.; Yu, L.; Zheng, Q. Anti-proliferation effects of licochalcone B on human breast cancer MCF-7 cells. Zhongguo Shiyan Fangjixue Zazhi 2016, 22, 106–111.
47. Kang, T.H.; Yoon, G.; Kang, I.-A.; Oh, H.-N.; Chae, J.-I.; Shim, J.-H. Natural compound licochalcone B induced extrinsic and intrinsic apoptosis in human skin melanoma (A375) and Squamous cell carcinoma (A431) cells. Phytother. Res. 2017, 31, 1858–1867.
48. Cho, J.J.; Chae, J.-I.; Yoon, G.; Ki, M.K.H.; Cho, J.H.; Cho, S.-S.; Cho, Y.S.; Shim, J.-H. Licochalcone A, a natural chalconoid isolated from Glycyrrhiza inflata root, induces apoptosis via Sp1 and Sp1 regulatory proteins in oral squamous cell carcinoma. Int. J. Oncol. 2014, 45, 667–674.
49. Oh, H.-N.; Yoon, G.; Shin, J.-C.; Park, S.-M.; Cho, S.-S.; Cho, J.H.; Lee, M.-H.; Liu, K.D.; Cho, Y.S.; Chae, J.-I.; et al. Licochalcone B induces apoptosis of human oral squamous cell carcinoma through the extrinsic- and intrinsic-signaling pathways. Int. J. Oncol. 2016, 48, 1749–1757.
50. Oh, H.-N.; Seo, J.-H.; Lee, M.-H.; Kim, C.; Kim, E.; Yoon, G.; Cho, S.-S.; Cho, Y.S.; Choi, H.W.; Shim, J.-H.; et al. Licochalcone C induces apoptosis in human oral squamous cell carcinoma cells by regulation of the JAK2/STAT3 signaling pathway. J. Cell. Biochem. 2018, 119, 10118–10130.
51. Oh, H.-N.; Oh, K.B.; Lee, M.-H.; Seo, J.-H.; Kim, E.; Yoon, G.; Cho, S.-S.; Cho, Y.S.; Choi, H.W.; Chae, J.-I.; et al. JAK2 regulation by licochalcone H inhibits the cell growth and induces apoptosis in human oral squamous cell carcinoma. Phytomedicine 2019, 52, 60–69.
52. Szliszka, E.; Czuba, Z.P.; Mazur, B.; Sedek, L.; Paradysz, A.; Krol, W. Chalcones enhance TRAIL-induced apoptosis in prostate cancer cells. Int. J. Mol. Sci. 2010, 11, 1–13.